Recirculating-Planar-Magnetron Simulations and Experiment

Matthew A. Franzi, Ronald M. Gilgenbach, *Fellow, IEEE*, Brad W. Hoff, *Member, IEEE*, David A. Chalenski, David Simon, Y. Y. Lau, *Fellow, IEEE*, and John Luginsland, *Member, IEEE*

***Abstract*—Microwave oscillation has been measured for the first time in a 12-cavity axial-magnetic-field recirculating planar magnetron, designed to operate in π mode at 1 GHz. The device operates with a −300-kV pulsed cathode voltage and a 0.2-T axial magnetic field, and oscillates at transverse currents exceeding 1 kA when driven by an electron beam pulselength between 0.5 and 1 μs. Microwave pulses were measured at frequencies between 0.97–1 GHz and achieved several hundred nanoseconds in length. Mode competition was observed between the π and 5 π/6 modes.**

***Index Terms*—Cavity magnetron, high power microwave, recirculating planar magnetron (RPM), vacuum electronics.**

I. Introduction

MAGNETRONS are efficient microwave generators, whose versatility and robust operation facilitate the device's extensive use in both military and commercial operations. This compact device is well suited for applications such as radar, counterelectronics, long-range communication, and commercial heating [1]–[5]. Since the device's inception in 1940, the resonant cavity magnetron has seen continuous advancement in both power output and efficiency [4], [5]. These improvements, however, do not address the inherent limitations of the device's geometry [6].

Conventional cylindrical magnetrons are susceptible to relatively limited diode currents due to small cathode area. Limited diode currents may hinder both average and peak output power. Low-impedance high-current structures can be attained but at cost of a significant increase in the cross-sectional area, the number of cavities, and the volume of the magnetic field. Conversely, inverted magnetrons are comparatively limited in the anode area, which hampers the heat removal and the number of viable power extractors. Planar magnetrons, which provide large surface areas and ideal power/volume scaling, are inefficient in comparison due to lack of recirculation and substantial losses in beam dumps or collectors.

The recirculating planar magnetron (RPM) [6], [7] is a crossed-field device that combines the advantages of high-efficiency recirculating devices with those of planar devices, i.e., both large-area cathode (high current) and anode (improved thermal management). Additionally, the magnetic-field volume of the RPM scales with N as compared with N^2 for cylindrical magnetron, where N is the number of cavities. Two embodiments of the RPM are the following: 1) the axial magnetic field with the radial electric field and 2) the radial magnetic field with axial electric field.

The primary focus of this paper will be the validation of the RPM's dispersion relation and operational feasibility through theory and experiment using the first type, with an axial magnetic field, shown in Fig. 1. Output coupling and high efficiency microwave power extraction are not included in this preliminary paper.

Alternate configurations of the RPM, not discussed in this paper, include the inverted polarity design and a continuous slow-wave structure design with cavities along the cylindrical sections [6].

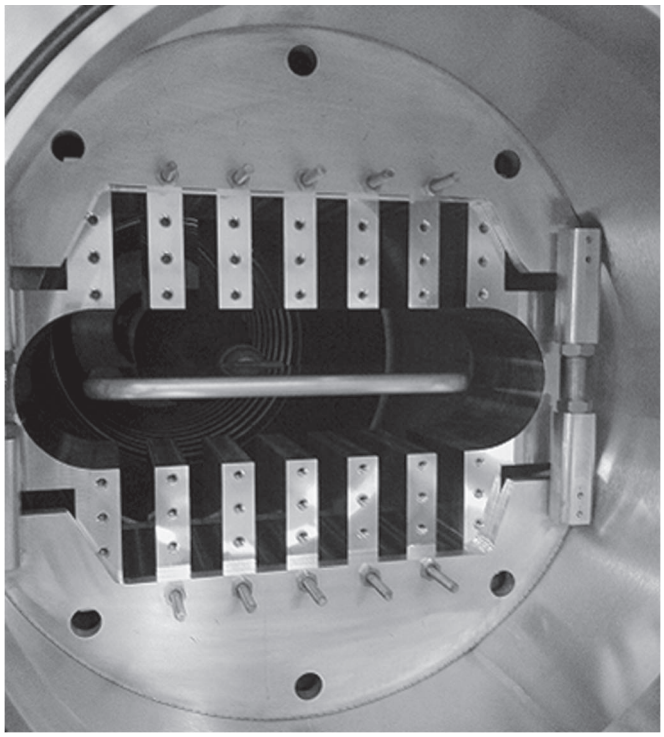

Fig. 1. Photograph of the RPM-12a experiment viewed from the front of the vacuum chamber. The center plate is the cathode, the anode periodic structures are above and below the cathode, and the axial magnetic field points out of the page.

Manuscript received October 3, 2012; revised December 17, 2012; accepted January 4, 2013. Date of publication March 7, 2013; date of current version April 6, 2013. This work supported in part by the Air Force Office of Scientific Research under Grant FA9550-10-1-0104, by the Air Force Research Laboratory, and by L-3 Communications Electron Devices.

M. A. Franzi, R. M. Gilgenbach, D. A. Chalenski, D. Simon, and Y. Y. Lau are with the Plasma, Pulsed Power, and Microwave Laboratory, University of Michigan, Ann Arbor, MI 48109-2104 USA.

B. W. Hoff is with the Air Force Research Laboratory, Kirtland Air Force Base, Albuquerque, NM 87117 USA.

J. Luginsland is with the Air Force Office of Scientific Research, Arlington, VA 22203 USA.

Digital Object Identifier 10.1109/TPS.2013.2242493

II. Theory and Design

The RPM consists of four distinct structural elements, i.e., two planar slow-wave structures with rectangular cavities and two smoothbore, adjoining cylindrical sections to provide beam recirculation.

The planar slow-wave structure is designed to support a π-mode electric-field configuration at a given operational frequency [2]–[5]. The basic configuration is simplified to periodic rectangular cavities equally spaced between rectangular vanes.

An infinite series of identical planar resonators is analyzed, with period L, the anode-cathode gap b, the cavity depth h, the cavity width w, and the phase velocity ω/β_0, where ω is frequency and β_0 is the fundamental propagation constant for planar magnetron. The initial design of the RPM is simplified by assuming equally spaced vanes and cavities such that the period of the slow-wave structures, composed of one vane of width w and one cavity of width w, may be represented as $L = 2w$. Assuming a uniform electric field between the planar vanes, terms $\beta_n = \beta_0 + 2\pi$n/L and $\gamma_n = \sqrt{\beta_n^2 - (\omega/c)^2}$ (c is the speed of light) are introduced to account for the superposition of higher order space harmonics. The resultant dispersion relation may be numerically solved as [8], [9]

$$\cot\left(\frac{\omega \boldsymbol{h}}{c}\right) = \sum_{n=-\infty}^{n=\infty} \frac{\omega}{\gamma_n c}\left(\frac{w}{L}\frac{\sin\left(\frac{\beta_n w}{2}\right)}{\frac{\beta_n w}{2}}\coth(\gamma_n b)\right). \quad (1)$$

The applied electric and magnetic fields necessary to achieve synchronism between the beam and the RF wave of the RPM are estimated using the Brillouin flow model for a smooth bore diode in Cartesian coordinates [10]–[12]. The relativistic Hull cutoff voltage V_h and the Bunemann-Hartree condition, shown in (2) and (3), respectively, are uniquely determined by setting the applied magnetic field B, the anode height b, the cathode height a, and phase velocity β (in units of c). For planar magnetron, the following are the same for the Brillouin flow model and the single particle model [10]–[12]:

$$\frac{eV_{\boldsymbol{h}}}{mc^2} = \left[1 + \frac{e^2B^2(b-a)^2}{m^2c^2}\right]^{\frac{1}{2}} - 1 \quad (2)$$

$$\frac{eV}{mc^2} = \frac{eB(b-a)}{mc}\beta - \left[1 - (1-\beta^2)^{\frac{1}{2}}\right]. \quad (3)$$

The RPM anode deviates from our ideal analytic assumption, i.e., of an infinite planar array, with the inclusion of cylindrical recirculation sections. The purpose of these smoothbore features is to maximize propagation of beam current from one oscillator to the other, which is analyzed using the metric of beam recirculation efficiency. Beam recirculation efficiency can be quantified in the simulation by observing the total current entering the cylindrical regime from one oscillator versus the total current leaving the same regime as it enters the opposing oscillator [see Fig. 4(a)]. Additional considerations for this recirculation region, such as RF feed through and space charge spoke preservation, are not analytically included for in this initial process. The anode radius is instead primarily selected to optimize recirculated current (electron hub heights below 80% of the AK gap) and match drift velocity of the planar slow-wave structure (0.2–0.3 c). Canceling the common factor (Λ) (where $\Lambda = (1/r_b)\sqrt{((kb)^2 + (\gamma\beta)^2)}$, the following are used to related the applied fields, the anode radius b, the cathode radius a, and the beam velocity in units of c (β) to the electron hub height r_b for a smooth bore Brillouin flow (γ is the relativistic factor) [10]–[12]:

$$\frac{eV}{mc^2} = \gamma - 1 + r_b\beta\gamma\ln\left(\frac{b}{r_b}\right)\Lambda \quad (4)$$

$$B\frac{e(b-a)}{mc} = \frac{1}{(b+a)r_b}\left(\left(b^2 - r_b^2\right)r_b\gamma\Lambda + \left(r_b^2 + b^2\right)\gamma\beta\right). \quad (5)$$

A. Design Parameters

A 1-GHz, 12-vane prototype RPM was designed and constructed assuming applied voltages in the range of -250 to -300 kV and a 0.15- to 0.2-T axial magnetic field. A 12-cavity model was chosen (six cavity-vane pairs on either planar side) to balance the mode competition with the peak power [2].

Initial designs utilized a thin cathode, which is 1.27-cm thick, to mitigate plasma expansion and diode closure. The initial cathode (Cathode-LC1) is centered within the anode, shown in Fig. 1, forming a 3.83-cm AK gap and spanning 24.3 cm in length to house the six cavities. The depth of the resonant cavities were set to 6.31 cm to achieve the π-mode resonance at the design output frequency of 1-GHz. Vanes and cavities have equal thickness $w = 1.92$ cm; the slow-wave structure period $L = 2w = 3.84$ cm. Consequently, the wavelength of the π-mode is $2L = 7.86$ cm with the corresponding phase velocity $v_{\rm ph}/c = 2Lf/c = 0.26$. The radius of the anode was set at 4.45 cm in order to maintain an estimated electron beam velocity between 0.25 and 0.3 c, as well as limit the cylindrical electron hub height to approximately half the AK gap to enhance recirculation efficiency. The anode block was designed to inhibit the development of axial modes by limiting the axial length to 11 cm, well below a half-free-space wavelength (15 cm).

III. Simulations and Cold Tests

The RPM-12a structure was rendered as an unloaded 3-D model in the finite-element-solver High-Frequency Structure Simulator (HFSS) [13]. Using the eigenmode solution routine, axially uniform π and $5\pi/6$ modes were identified at 1.01 and 0.988 GHz, respectively. These simulated results were experimentally verified in cold-test measurement using a dipole antenna, oriented parallel to the array of planar cavities. The antenna, in conjunction with a 6772D Agilent frequency sweeping network analyzer, was used to perform a frequency sweep from 850 to 1050 MHz with 125-kHz resolution. The resultant single-port (S_{11}) data, shown in Fig. 2, demonstrates strong agreement with simulated resonant modes; 1.008 $(Q = 1740)$ and 0.984 GHz $(Q = 590)$ correlate well to the π and $5/6\pi$ modes, respectively, found in the HFSS. The identification of the modes is presented in Table I.

Degenerate or phase-shifted equivalent modes in a cylindrical magnetron are usually negligible due to the azimuthal

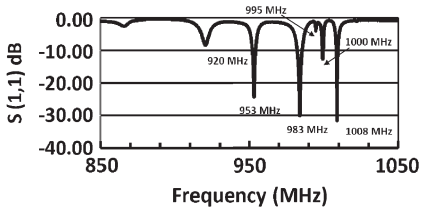

Fig. 2. Experimental $S(1,1)$ parameter of a dipole antenna inside the resonant RPM cavity. Modes identified in Table I.

TABLE I
COMPARISON OF SIMULATED VERSUS EXPERIMENTAL COLD TEST OF THE RPM CAVITY

Mode	π/2	2π/3	5π/6	Π
HFSS (GHz)	0.945	0.965	0.988	1.01
Antenna (GHz)	0.92	0.953	0.983	1.008

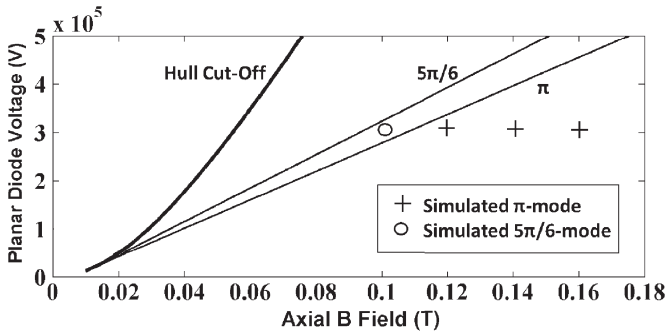

Fig. 3. Simulated oscillating modes plotted versus Bunemann-Hartree resonance and Hull cutoff conditions for the RPM-12a planar diode.

symmetry of both the device and the mode [2]. The RPM, in contrast, experiences a geometrical discontinuity at the planar-cylindrical interface. Phase-shifted modes, which are no longer fully symmetric but have the same planar propagation constant, consequently experience a spread in frequency. RPM-12a demonstrates a twofold degeneracy in most operating modes, where the position of nodes and antinodes are interchanged. These separate and competing modes are classified as even (0° phase shift) or odd (180° phase shift) between mirrored cavities on the top versus bottom oscillators. The spatially degenerate π and $5\pi/6$ modes were identified in the HFSS at frequencies of 1.012 and 0.999 GHz, respectively. While either π-mode would result in the optimal planar operation, there exists mode competition between them, which can adversely affect the operation of the RPM.

A 3-D model of the full experimental setup for RPM-12a was simulated using the electromagnetic particle in cell code MAGIC. A -250-kV voltage pulse was imposed on the cathode stalk, and the magnetic field was varied between 0.1 and 0.16 T, in order to produce electron beam drift velocities in the vicinity of π-mode phase velocities $(v_{\rm ph} \sim 0.26c)$, for durations of 200ns. The resultant modes of operation for this device may be estimated using the Brillouin flow theory, illustrated in Fig. 3.

Simulations with an applied B field equal to 0.12, 0.14, and 0.16 T, which theoretically yielded drift velocities slightly below 0.26 c, produced π-mode oscillations at 1.002 GHz,

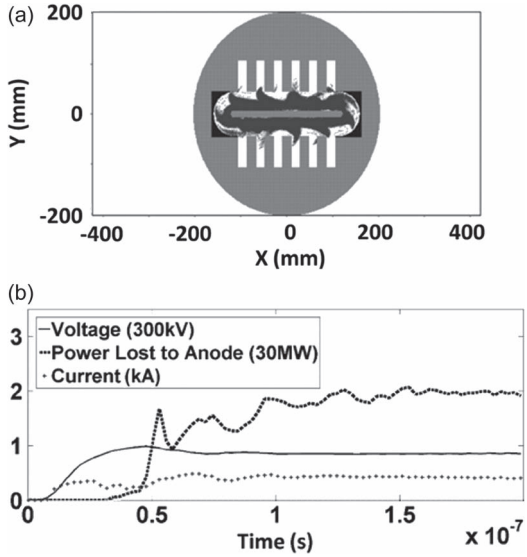

Fig. 4. (a) MAGIC particle-in-cell 3-D phase space profile of RPM-12a in the π-mode operation. (b) Simulated voltage, current, and net power of electrons impacting the anode using MAGIC 3-D (Bo $= 0.12$ T).

while the case run using $B = 0.10$ T, which exceeded the π-mode threshold, operated in the $5\pi/6$ mode at a frequency of 0.975 GHz. Operating at magnetic fields below 0.10 T demonstrated significant losses to the anode as the Hull cutoff condition is quickly reached.

A closer examination of these simulated runs using the 0.12-T applied magnetic-field case, as an example of the π-mode operation, is presented in Fig. 4(a) and (b). Using "endhat" structures to inhibit electrons from leaving the AK gap, the simulation demonstrated that of the 3 kA emitted from the cathode, approximately 2.6-kA average current returned to the cathode; the remaining 400 A was primarily lost to the anode structure. The net power of these electrons impacting the anode reached nearly 60 MW or 63% of the 95-MW average input power, which is illustrated by the heavy dotted curve in Fig. 4(b). An additional 13 MW is lost between the resistive surface loss and the cathode heating, leaving an upper limit of 22 MW or ∼20% to be radiated as microwaves into the chamber before exiting the simulation through an output port axially downstream from the anode.

Beam recirculation, calculated by electron interception in the semi-circular sections in Fig. 4(a), was shown to exceed 98% under nominal operating conditions. Electrons in the planar regions reach the synchronous drift velocity (0.26 c) at approximately 1.8 cm above the cathode (∼50% of the AK gap). The density of electrons past this point decays toward the RPM anode.

IV. EXPERIMENTAL CONFIGURATION

The Michigan Electron Long Beam Accelerator, with a ceramic insulator stack, (MELBA-C) drives the RPM at -300 kV for pulselengths between 0.3 and 1 μs [14].

Fig. 5 depicts the experimental configuration for the RPM. Time-resolved voltage and entrance current measurements are made using a copper sulfate $(CuSO_4)$ resistive divider and an

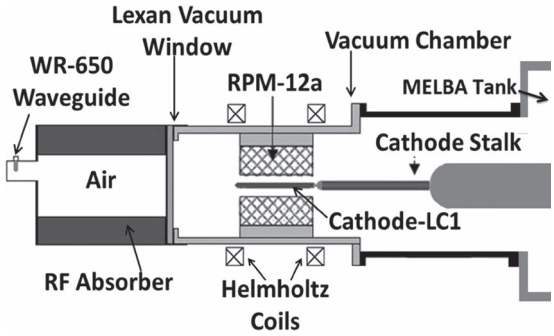

Fig. 5. Experimental RPM equipment diagram (right) from pulse generator MELBA (left) to the RF load.

embedded Rogowski coil in the wall of the vacuum chamber, respectively. Pulsed concentric electromagnets are spaced approximately 21.6 cm apart to form an approximate Helmholtz pair and provide a nearly uniform axial magnetic field, adjustable between 0.1 and 0.3 T. In the Helmholtz magnetic-field configuration, B varies in magnitude with respect to radial distance from the central axis of the electromagnets. The resultant decrease in the magnetic field from the center of the device to the exterior recirculation region was found to be approximately 10% of the peak on-axis field. Simulations using this realistic magnetic-field profile have shown a negligible impact on the overall operation and recirculation efficiency.

The #304 stainless steel vacuum chamber, which 63.5 cm in length, has an inner diameter of 39.4 cm and, with cryopumping, is capable of sustaining vacuum between 9×10^{-7} and 4×10^{-6} torr. The chamber terminates into a transparent 2.54-cm-thick, Lexan window, which seals to an O-ring interface on the outer most flange. The inner surface of the copper load chamber is coated with an 8-cm-thick annulus of microwave absorber (Ecosorb) in order to dissipate microwave power outside of the vacuum system. Single-port simulations performed in the HFSS indicate a return loss of -15 dB at 1 GHz.

The experimental anode prototype RPM-12a is centered in the vacuum chamber with the Cathode-LC1 extending into the midplane between the planar slow-wave structures. Dielectric fibers were attached to the cathode in 10-cm strips approximately 1.9 cm wide to match the width of the anode vanes. A total of six strips, with three placed underneath every other vane on both sides of the cathode, were used to enhance π-mode oscillations via cathode emission priming [15].

The open-cavity configuration of the RPM allows for generated microwave pulses to freely radiate (albeit inefficiently) into the vacuum chamber from both sides of the anode via diffraction coupling [16]. Microwave pulses traverse out of the vacuum chamber, through the Lexan window, into the load chamber before coupling to a WR650 waveguide with type-N receiving antenna into RG-213U coaxial cable. The signal is processed in the Faraday cage using a series of type-N attenuators between 40 to 55 dB down before being split and input to separate frequency and power diagnostics. Frequency is observed using heterodyne detector, which mixes the attenuated microwave pulse with a 1.2-GHz 10-dBm continuous-wave signal from an Agilent E4422B signal generator. The attenuated microwave signal is rectified by a calibrated Agilent 8472B diode detector, from which the RPM power is established.

Axial electron endloss was measured by a Pearson coil (Model 410) connected to a (36.6 cm X 10.2 cm) current collector mounted on the inside of the Lexan window.

V. Experimental Results

The RPM was pulsed at voltages between -250 and -300 kV with externally applied axial magnetic fields in the range of 0.18 to 0.2 T over 500 to 700-ns pulselengths. Microwave pulselengths of several hundred nanoseconds were consistently generated with microwave oscillation start times between 150 and 300 ns, if the "start-oscillation" current threshold was reached. The average total current emission was between 2 and 4 kA during microwave oscillation including endlosses. The electron endloss measured out one end of the cathode was typically 20%–25% of the total current during peak microwave power. The total electron endloss is anticipated to reach nearly twice this value when considering similar losses from the nearly symmetric outlet on the other side of the device. Using this assumption for extrapolating the total endloss out of the entire device, the transverse electron current in the device, at start oscillation, would be in the range of 1–2 kA. The spectrum of generated microwaves consisted of three primary frequencies at 0.98, 1.01, and 1.015 GHz corresponding to $5\pi/6$, even-π, and odd-π modes.

The shot data, shown in Fig. 6(a), display the typical π-mode operation of the RPM for 250 ns at an average voltage of -250 kV and 0.2-T axial magnetic field. The average total current during oscillation remained fairly constant at 3.3 kA; the transverse electron current is estimated to be 1.3 kA. Mild microwave power modulation and wave beating, which are evident in the discontinuous contour in Fig. 6(b) and neighboring modes in Fig. 6(c), are attributed to the weak coupling of dissimilar operating frequencies between the top and bottom oscillators. Discrepancies in the operating frequency, on the order of a few megahertz, may develop from nonuniform charge density and beam loading or the development of out-of-phase or degenerate modes previously discussed.

A case of severe mode competition is demonstrated in Fig. 7(a)–(c). Plasma expansion and subsequent closure of the AK gap caused the total emitted current to increase from approximately 3 kA at startup to a total peak current of 4.2 kA (estimated transverse current of 2.2 kA) when the microwave oscillation ceased. The unstable oscillating mode can be attributed to both the closely spaced mode structure and the dynamic changes in the current density and the effective AK gap of the RPM. The failure of the cavities to lock to a single frequency also caused a substantial drop in sampled microwave power.

Mode competition may also result in dual frequency "mode hopping" or bimodal shot profiles [3]. The Fourier transform shown in Fig. 8 displays strong competition between neighboring $5\pi/6$ (0.988 GHz) and odd-π modes (1.015 GHz).

RPM-12a, at these electric and magnetic fields, was highly susceptible to mode competition and demonstrated a lack of consistency in producing a single operating mode on a

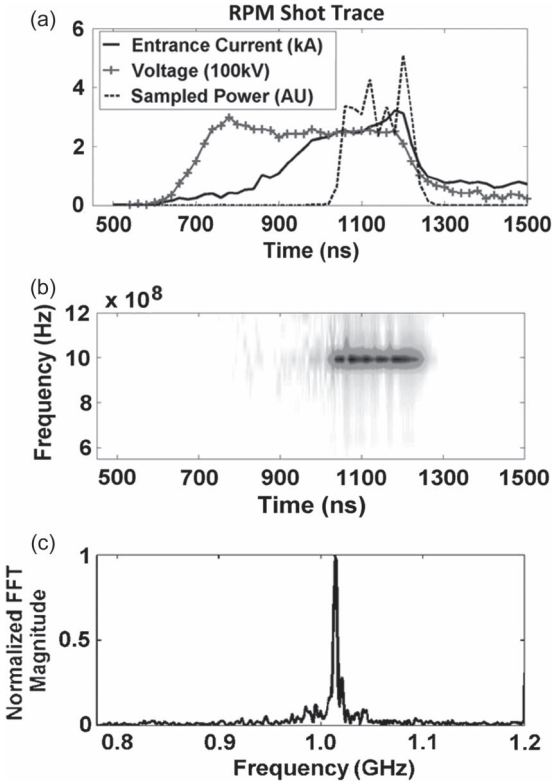

Fig. 6. (a) Experimental RPM shot data. (b) Heterodyne time_frequency analysis (black = highest signal strength). (c) Fast Fourier transform over the entire microwave pulse.

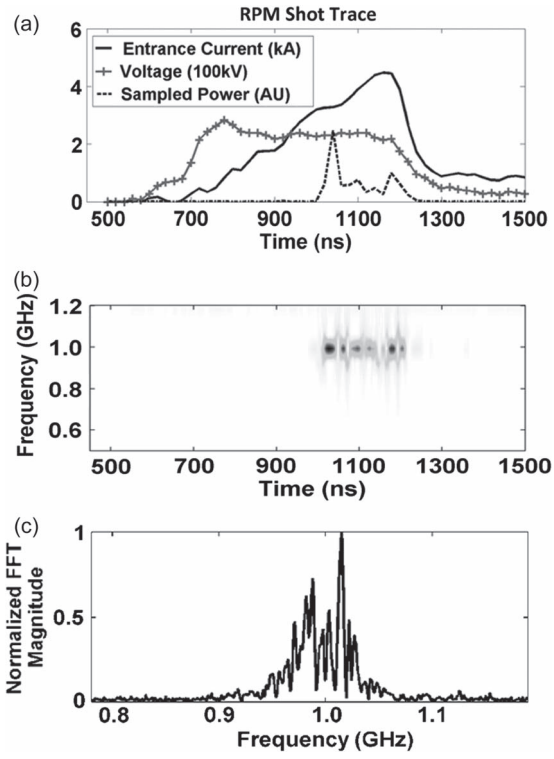

Fig. 7. (a) Experimental RPM shot data. (b) Heterodyne time_frequency analysis (black = highest signal strength). (c) Fast Fourier transform over the entire microwave pulse.

shot-to-shot basis. A summary of the π-mode, $5\pi/6$-mode, and bimodal results are shown in Fig. 9, representing all of the shots on RPM-12a.

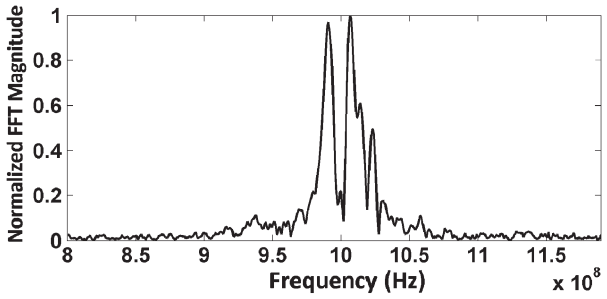

Fig. 8. Time-integrated fast Fourier transform demonstrating the bimodal operation of RPM-12a.

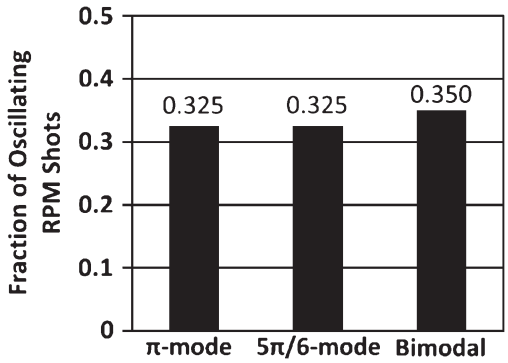

Fig. 9. Quantitative summary of operating modes for all experimental RPM-12a shots at applied fields of -250 kV and 0.2 T.

The sampled microwave power measurements were only used for mode identification and the timing of generated radiation. Calibrated experimental extracted power measurements are not included in this paper, as there was no guided extraction mechanism included in the prototype anode (a subject of future research).

VI. Conclusion and Future Research

The RPM represents a novel adaptation of the modern cavity magnetron, which holds numerous geometrical advantages over purely cylindrical or planar systems. This paper has described the design and the operation of an L-band prototype with 12-vane dual-linear six-cavity arrays. The AK gap (3.83 cm), the π-mode frequency (1.01 GHz), and the π-mode phase velocity (0.26 c) were selected to match the pulsed driver MELBA-C at approximately -300-kV pulsed cathode voltage.

The primary goal of these experiments has been to generate microwave oscillation in the RPM and to interpret the data in terms of the analytic dispersion relation. Results have demonstrated that the device is capable of producing microwave radiation at a specifically designed π-mode frequency but is highly susceptible to mode competition from neighboring operating modes. Further simulations and experiments are being performed to mitigate mode competition and enhance startup including anode strapping, cathode emission priming, planar "rising sun" cavity configurations, reducing the number of cavities in each oscillator, and mode control through novel cathode structures. Advanced cathodes will also include end-loss inhibitors (endcaps), which are also anticipated to improve overall efficiency.

Future recirculating planar magnetron research will concentrate on microwave extraction techniques to improve the electronic efficiency to values competitive with previous relativistic magnetron experiments [3], [14].

REFERENCES

[1] T. A. Spencer, "Current HPM source research," in *Proc. 6th Workshop High Energy Density High Power RF*, Berkeley Springs, WV, 2003, p. 46.

[2] G. B. Collins, *Microwave Magnetrons*. New York, NY, USA: McGraw-Hill, 1948.

[3] R. M. Gilgenbach, Y. Y. Lau, H. McDowell, K. L. Cartwright, and T. A. Spencer, *Crossed-Field Devices*, R. J. Barker, N. C. Luhmann, J. H. Booske, and G. S. Nusinovich, Eds. Piscataway, NJ, USA: IEEE Press, 2004, ch. Chapter 6 in Modern Microwave and Millimeter Wave Power Electronics.

[4] A. S. Gilmour, *Microwave Tubes*. Norwood, MA, USA: Artech House, 1986, pp. 348–379.

[5] J. Benford, J. A. Swegle, and E. Schamiloglu, *High Power Microwaves*. Boca Raton, FL, USA: CRC Press, 2007.

[6] R. M. Gilgenbach, Y. Y. Lau, D. M. French, B. W. Hoff, M. Franzi, and J. Luginsland, "Recirculating planar magnetrons for high-power high-frequency radiation generation," *IEEE Trans Plasma Sci.*, vol. 39, no. 4, pp. 980–987, Apr. 2011.

[7] R. M. Gilgenbach, Y. Y. Lau, D. M. French, B. W. Hoff, and M. Franzi, "Crossed field device," U.S. 2011/0204785 A1, Aug. 25, 2011, Patent Pending.

[8] Y. Y. Lau and D. Chernin, "A review of ac space charge effect in electron circuit interactions," *Phys. Fluids B*, vol. 4, no. 11, pp. 3473–3497, Nov. 1992.

[9] J. W. Gewartowski and H. A. Watson, *Principles of Electron Tubes: Including Grid-Controlled Tubes, Microwave Tubes, and Gas Tubes*. New York, NY, USA: Van Nostrand, 1965.

[10] R. C. Davidson, G. L. Johnston, K. T. Tsang, and A. T. Drobot, "Cylindrical Brillouin flow in relativistic smooth-bore magnetrons," in *Proc. SPIE Conf. Ser.*, 1989, vol. 1061, pp. 186–200.

[11] Y. Y. Lau, J. W. Luginsland, K. L. Cartwright, D. H. Simon, W. Tang, B. W. Hoff, and R. M. Gilgenbach, "A re-examination of the Buneman_Hartree condition in a cylindrical smooth-bore relativistic magnetron," *Phys. Plasmas*, vol. 17, no. 3, pp. 033102-1–033102-9, Mar. 2010.

[12] D. H. Simon, Y. Y. Lau, J. W. Luginsland, and R. M. Gilgenbach, "An unnoticed property of the cylindrical relativistic Brillouin flow," *Phys. Plasmas*, vol. 19, no. 4, pp. 043103-1–043103-5, Apr. 2012.

[13] [Online]. Available: http://www.ansoft.com/products/hf/hfss/

[14] M. R. Lopez, R. M. Gilgenbach, M. C. Jones, W. M. White, D. W. Jordan, M. D. Johnston, T. S. Strickler, V. B. Neculaes, Y. Y. Lau, T. A. Spencer, M. D. Haworth, K. L. Cartwright, P. J. Mardahl, J. W. Luginsland, and D. Price, "Relativistic magnetron driven by a microsecond E-beam accelerator with a ceramic insulator," *IEEE Trans. Plasma Sci.*, vol. 32, no. 3, pp. 1171–1180, Jun. 2004.

[15] M. C. Jones, V. B. Neculaes, Y. Y. Lau, R. M. Gilgenbach, and W. M. White, "Cathode priming of a relativistic magnetron," *Appl. Phys. Lett.*, vol. 85, no. 26, pp. 6332–6334, Dec. 27, 2004.

[16] M. I. Fuks, N. F. Kovalev, A. D. Andreev, and E. Schamiloglu, "Mode conversion in a magnetron with axial extraction of radiation," *IEEE Trans. Plasma Sci.*, vol. 34, no. 3, pp. 620–626, Jun. 2006.

Matthew A. Franzi received the B.S. and M.S.E. degrees from the University of Michigan, Ann Arbor, MI, USA, in 2008, and 2010, respectively, where he is currently working toward the Ph.D. degree.

He is a Graduate Research Assistant with the Plasma, Pulsed Power, and Microwave Laboratory, University of Michigan, working on radio-frequency source development and conditions for stimulating multipactor breakdown under Prof. R. Gilgenbach.

Ronald M. Gilgenbach (M'74–SM'92–F'06) received the B.S. and M.S. degrees from the University of Wisconsin, Madison, WI, USA, in 1972 and 1973, respectively, and the Ph.D. degree in electrical engineering from Columbia University, New York, NY, USA, in 1978.

In the early 1970s, he spent several years as a Member of the Technical Staff with Bell Laboratories. From 1978 to 1980, he performed gyrotron research with the Naval Research Laboratory and performed the first electron cyclotron heating experiments on a tokamak plasma in the USA with the Oak Ridge National Laboratory. Since 1980, he has been with the faculty of the University of Michigan (UM), Ann Arbor, MI, USA, where he is the Director of the Plasma, Pulsed Power, and Microwave Laboratory, and the Chair and the Chihiro Kikuchi Collegiate Professor with the Department of Nuclear Engineering and Radiological Sciences. With the UM, He has supervised 45 Ph.D. students. He has published over 160 articles in refereed journals. He is the holder of four patents and has a fifth application filed. He has collaborated in research with scientists at the Air Force Research Laboratory, Sandia National Laboratories, the National Aeronautics and Space Administration Glenn, Northrop–Grumman, L-3 Communications, the General Motors Research Laboratories, Los Alamos National Laboratory, Fermilab, the Naval Research Laboratory, and the Institute of High Current Electronics (Russia).

Dr. Gilgenbach was a recipient of the 1984 National Science Foundation Presidential Young Investigator Award and the 1997 Plasma Sciences and Applications Committee (PSAC) Award from the IEEE. He served as PSAC Chair from 2007 to 2008. He is a Fellow of the American Physical Society Division of Plasma Physics. He is a past Associate Editor of the Physics of Plasmas journal.

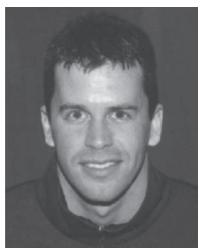

Brad W. Hoff (S'04–M'10) received the B.S. degree in physics from the U.S. Naval Academy, Annapolis, MD, USA, in 1999 and the M.S.E. degree in nuclear engineering, the M.S.E. degree in electrical engineering, and the Ph.D. degree in nuclear engineering from the University of Michigan, Ann Arbor, MI, USA, in 2006, 2007, and 2009, respectively.

He is currently a Research Physicist with the Directed Energy Directorate, Air Force Research Laboratory, Kirtland Air Force Base, Albuquerque, NM, USA. His research interests include high-power microwave sources and directed energy technology.

David A. Chalenski was born in Syracuse, NY. He received the B.S., M.S., and Ph.D. degrees from Cornell University, Ithaca, NY, USA, in 2004, 2009 and 2010, respectively.

While with Cornell University, he studied wire array z-pinches and pulsed-power technology with the Laboratory of Plasma Studies. Upon graduating, he continued a postdoctoral fellowship with Cornell University, studying planar laser-induced fluorescence on gas puff z-pinches. He is currently an Assistant Research Scientist with the Plasma Physics, Pulsed Power and High Power Microwave Laboratory, University of Michigan, Ann Arbor, MI, USA. He studies the seeded magneto-Rayleigh–Taylor instabilities on exploding foils using a megaampere linear transformer driver.

David Simon was born in Sacramento, CA. He received the double B.S. degree in mechanical engineering and nuclear engineering from University of California, Berkeley, CA, USA, in 2007. He is currently working toward the Ph.D. degree at the University of Michigan, Ann Arbor, MI, USA.

Y. Y. Lau (M'98–SM'06–F'08) was born in Hong Kong. He received the S.B., S.M., and Ph.D. degrees in electrical engineering from Massachusetts Institute of Technology (MIT), Cambridge, MA, USA in 1968, 1970, and 1973, respectively.

From 1973 to 1979, he was an Instructor and then an Assistant Professor in applied mathematics with MIT. He was a Research Physicist with Science Applications Inc., McLean, VA, USA, from 1980 to 1983 and the Naval Research Laboratory, Washington, DC, USA, from 1983 to 1992. Since 1992, he has been as a Professor in the applied physics program and with the Department of Nuclear Engineering and Radiological Sciences, University of Michigan, Ann Arbor, MI, USA. He is the holder of ten patents. He has over 190 refereed publications. He has worked on electron beams, coherent radiation sources, plasmas, and discharges. His recent interests include heating phenomenology, physics of quantum and higher dimensional diodes, Thomson X-ray sources, and electrical contacts.

Dr. Lau served three terms as an Associate Editor of the Physics of Plasmas and was a former Guest Editor of the IEEE TRANSACTIONS ON PLASMA SCIENCE Special Issue on High Power Microwave Generation. He was elected Fellow of the American Physical Society in 1986. He received the 1989 Sigma-Xi Scientific Society Applied Science Award and the 1999 IEEE Plasma Science and Applications Award.

John Luginsland (S'95–M'96) received the B.S.E., M.S.E., and Ph.D. degrees in nuclear engineering (plasma physics option) from the University of Michigan, Ann Arbor, MI, USA, in 1992, 1994, and 1996, respectively.

In 1996, he was a National Research Council Resident Research Associate with the Advanced Weapons and Survivability Directorate, Air Force Phillips Laboratory, and a Staff Member with the Plasma Physics Branch, Directed Energy Directorate, Air Force Research Laboratory, until 2001. From 2001 to 2003, he was with Science Applications International Corporation, where he was engaged in advanced pulsed-power applications. From 2003 to 2009, he was with NumerEx, Limited Liability Company, where his research interests included theoretical and computational plasma physics from the kinetic to magnetohydrodynamic limits, electromagnetism, and fluid dynamics with applications to advanced survivability concepts, accelerator schemes, combustion research, and various types of radiation production. Since 2009, he has been with the Air Force Office of Scientific Research, Arlington, VA, USA, where he is currently the Program Manager for fundamental research into plasma and electro energetic physics with focus areas in directed energy, nonequilibrium plasma, and high-energy density pulsed-power physics.

Dr. Luginsland is the Past Chair of the IEEE Nuclear and Plasma Sciences Society's (NPSS) Plasma Science and Applications Committee. He was the recipient of the 2006 IEEE NPSS Early Achievement Award.